doi: 10.56761/EFRE2022.S2-O-048501

Evolution of MITL parameters during the passage of a powerful current pulse

S.I. Tkachenko[1,2,3,], V.V. Aleksandrov[2], A.V. Branitskii[2], I.N. Frolov[2], E.V. Grabovskii[2], K.V. Khishchenko[1,3], K.N. Mitrofanov[2], G.M. Oleinik[2],*

[1]*Moscow Institute of Physics and Technology (National Research University), Dolgoprudny, Russia*
[2]*SRC RF TRINITI, Troitsk Moscow, Russia*
[3]*Joint Institute for High Temperatures, RAS, Moscow, Russia*
[*]*tkachenko@phystech.edu*

Abstract. Numerical modeling of the processes occurring in a cathode of vacuum transmission line during the passage of a powerful current pulse has been performed. The main parameters used in the numerical model correspond to the data of experiments carried out at the Angara-5-1 facility.
Keywords: numerical modeling, vacuum transmission line, powerful current pulse.

1. Introduction

The study of the processes occurring in matter under the influence of powerful energy flows on it is of great interest both for fundamental and applied sciences, and for various technologies. At the Angara-5-1 facility, extreme states of matter are studied when a powerful current pulse is passed through various loads [1–4]; linear current density in the load can reach 1 MA/cm. When a submicrosecond current pulse with a linear density of more than 1 MA/cm flows, a significant heating of the metal occurs, up to melting, evaporation, and ionization. To study the processes occurring in vacuum magnetically insulated transporting lines (MITL) when a current with a high linear density is passed through it, numerical calculations were carried out using a thick-walled tube as a MITL model.

2. Description of the model used in numerical calculations

A system of one-dimensional one-temperature magnetohydrodynamic equations was solved (in [2–4], a similar problem was studied for thin-walled tubes, the wall thickness of which was less than the skinning thickness of the magnetic field). The system of MHD equations used can be written as follows

$$\frac{dm}{dt} = 0, \tag{1}$$

$$\rho \frac{d\nu}{dt} = -\frac{\partial P}{\partial r} - \frac{0.5}{\mu r^2}\frac{\partial \left(r^2 B_\varphi^2\right)}{\partial r}, \tag{2}$$

$$\rho \frac{d\varepsilon}{dt} = -P\frac{\partial (rv)}{\partial r} + \frac{1}{r}\frac{\partial}{\partial r}\left(kr\frac{\partial T}{\partial r}\right) + \frac{j^2}{\sigma}, \tag{3}$$

$$\frac{d\left(\mu B_\varphi\right)}{dt} = \frac{\partial}{\partial r}\left(\frac{1}{\sigma r}\frac{\partial \left(rB_\varphi\right)}{\partial r}\right), \tag{4}$$

where m is the mass; ρ is the density of matter; v is the velocity; T is the temperature; B_φ is induction of magnetic field; $\sigma(\rho,T)$, $\kappa(\rho,T)$, $\varepsilon(\rho,T)$ and $P(\rho,T)$ are the conductivity, heat conductivity, specific internal energy and pressure correspondingly; $j = (\mu r)^{-1}\partial(rB_\varphi)/\partial r$ is the current density and μ is magnetic permeability.

The initial as well as boundary conditions on the inner and outer surfaces of the tube can be written

$$\rho(r,0) = \rho_0,\ T(r,0) = T_0,\ v(r,0) = 0,\ B_\varphi(r,0) = 0, \tag{5}$$

$$v(r_s,t) = dr_s/dt\ ,\ B_\varphi(r_{out},t) = \mu I(t)/2\pi r_{out}\ ,\ B_\varphi(r_{in},t) = 0\ ,\ P(r_s,t) = 0\ , \tag{6}$$

here, r_{in} and r_{out} are inner and outer radii of tube; r_s is one of these radii. To consider the evaporation of the substance from the surface of the tube r_s, we can write

$$k(\partial T/\partial r)\big|_{r=r_s} = \rho v_b(\Lambda - a_k R T_s/\mu_w)\ , \tag{7}$$

here, v_b is the velocity of the evaporation wave, Λ is the specific enthalpy of vaporization, R is the specific gas constant and T_s is the surface temperature. Coefficient a_k depends on the back pressure of medium near tube and in case of evaporation to vacuum $a_k = 0.77$ [5].

To describe the real properties of a substance, wide-range semi-empirical equations of state [6] were used, considering phase transformations (melting and evaporation) and the possibility of realizing metastable states, as well as the dependence of transport coefficients (conductivity and heat capacity) on temperature [2, 7].

The parameters of the tube made of stainless steel and the time dependence of the current in numerical modeling were used such that are similar to the experiments described in [8].

3. Results of numerical calculations

Fig.1 shows the time dependence of the current used in the simulation namely boundary condition (6) for magnetic field induction. The current was described by the dependence $I(t) = I_0 \cdot (\sin(\pi \cdot t/\tau_0))^2$, coefficients I_0 and τ_0 were chosen in such a way that the function $I(t)$ described the change in the current up to its amplitude value in the experiment, the results of which are presented in [8].

Fig.1 shows also the voltage curve calculated in accordance with the relationship $V = j \cdot \sigma \cdot l$ (here l is the tube length, j and σ are the current density and conductivity which obtained by numerical modeling at the inner surface of tube); we can see a peculiarity at ~100 ns marked with arrows in the figure. At this time the voltage grows more slowly than in the previous and subsequent moments. Analyzing the data obtained in the calculations (temperature and phase state), we can conclude that this feature corresponds to the exit of a melting wave on the inner surface of the tube and lasts (~5 ns) until the substance on the inner surface is completely melted. On the time dependence of the voltage measured in the experiment on the inner surface of the tube, there is also a feature with a lower rate of voltage increase, it lasts a little longer (~8 ns) and the rate of voltage change during this time is less than in numerical data [8]. The voltage value in this time, in accordance with the experimental data, is ~15 kV, and the value of ~11–12 kV was obtained in the calculations.

Due to the good agreement between the experimental and calculated data on this feature, it can be argued that the experimental time dependence of the voltage also shows the exit of a melting wave on the inner surface of the tube and the moment of completion of the melting of the tube substance.

After the end of the melting of the substance on the inner side of the tube, the voltage, in accordance with the experimental dependence, increases to ~20 kV, and in the calculations, it reaches ~16 kV. The time to reach the maximum voltage value, counted from the moment the current start, is 130 and 145 ns in experiments and calculations, respectively.

Fig.1 shows that the inner border of the tube has moved more than the outer one.

Fig.2 shows the distributions of pressure, temperature, substance density and current density over the wall thickness of a tube with an outer diameter of 3 mm and a wall thickness of 220 μm at 100 ns. It can be seen that by the time of 100 ns, the current density is almost uniformly distributed over the tube thickness, the substance density decreased most of all at the outer boundary of the tube in the region where the temperature increased the most. By this moment, the substance of the tube from the outer boundary and a little more than to the middle of its thickness is already in a

liquid state; the remaining inner part has not yet had time to completely melt and is in a two-phase state of solid–liquid. The maximum pressure is in the middle of the tube wall.

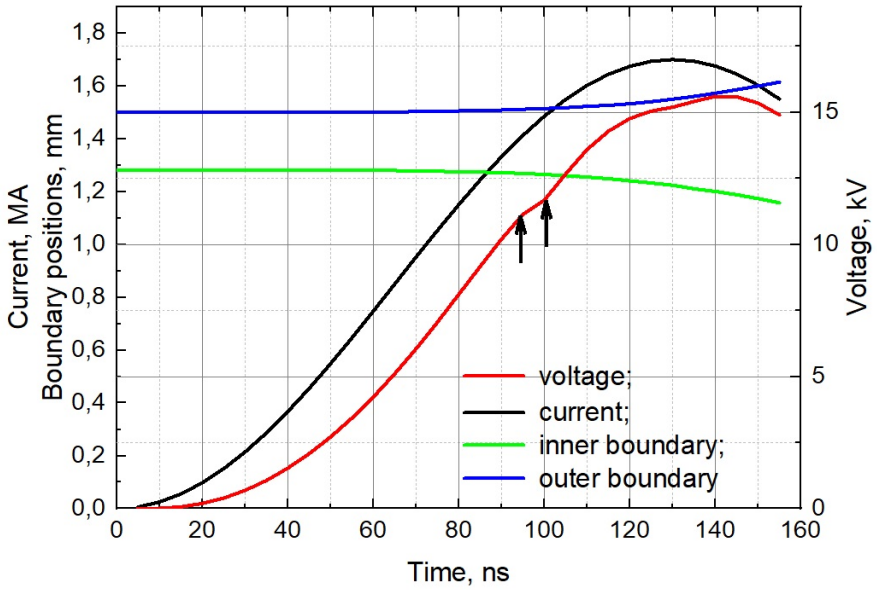

Fig.1. Time dependencies of the current and voltage on the upper part of the tube on its inner surface, as well as changes in the positions of the outer and inner boundaries of the tube. The arrows show the moments of the melting wave reaching the inner boundary of the tube and the completion of the melting process.

Fig.3–7 show the distributions of parameters over the tube thickness at different times. On these graphs, one can trace the evolution of the parameters of the tube substance from the moment the current is started until the moment it reaches its maximum value. During this time, the tube has time to completely melt and heat up to the near-critical temperature of iron, and some of its layers heat up to ~1 eV.

After decreasing the current (its peak value is reached at 130 ns), i.e., decreasing the magnetic field induction at outer surface (Fig.6), and, consequently, the current density and compressive magnetic pressure decrease, the outer layers of the tube begin to expand faster (see Fig.7), respectively, their temperature becomes somewhat lower than the temperature of the nearest inner layers (Fig.3).

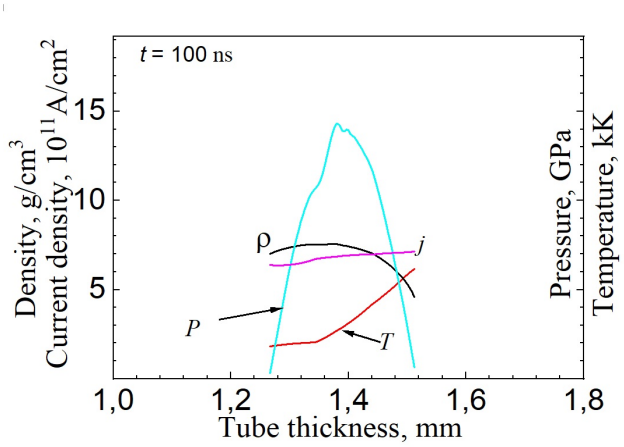

Fig.2. Distribution of pressure, temperature, mass density and current density over the thickness of a tube made of stainless steel.

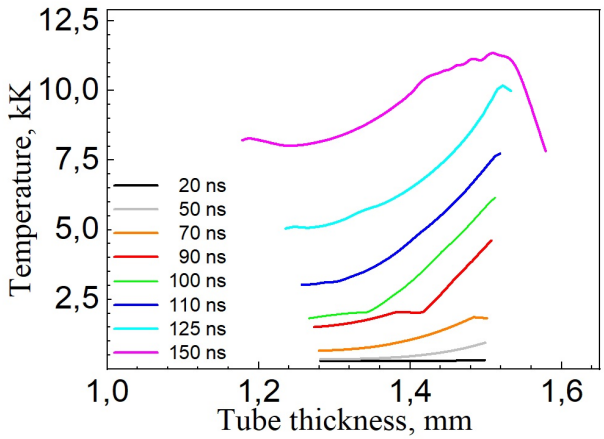

Fig.3. Temperature distribution over the tube thickness at different instants.

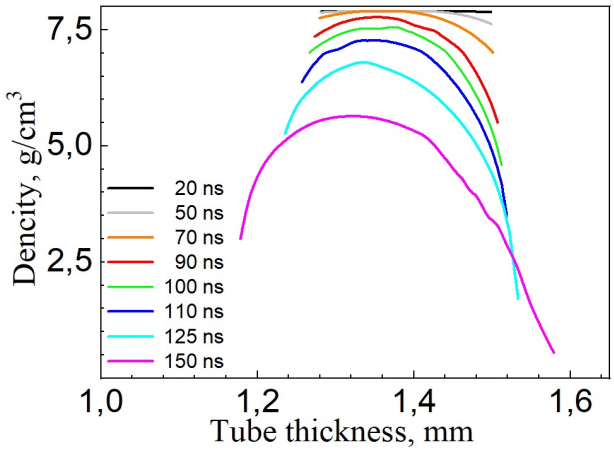

Fig.4. The distribution of the mass density over the thickness of the tube at different instants.

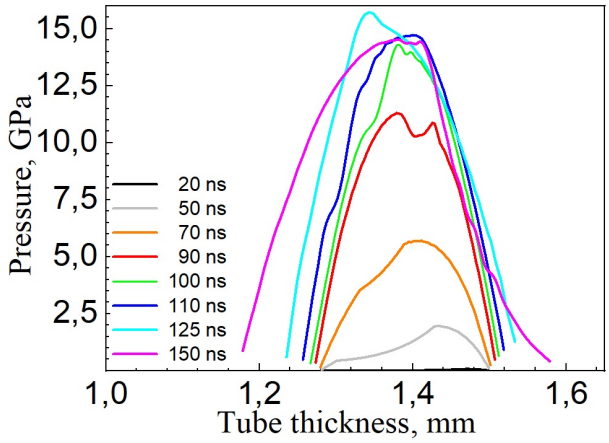

Fig.5. Distribution of pressure over the thickness of the tube at different instants.

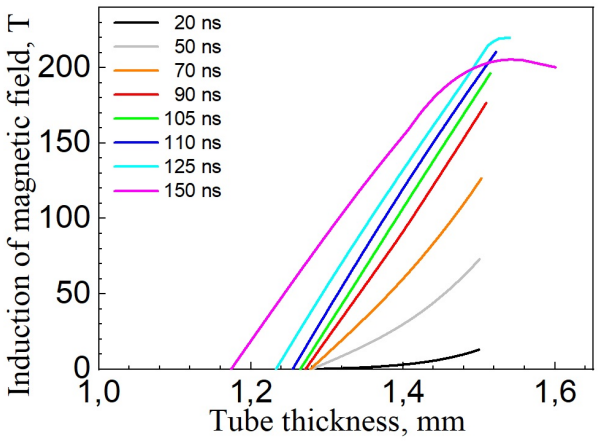

Fig.6. Distribution of the magnetic field induction over the thickness of the tube at different instants.

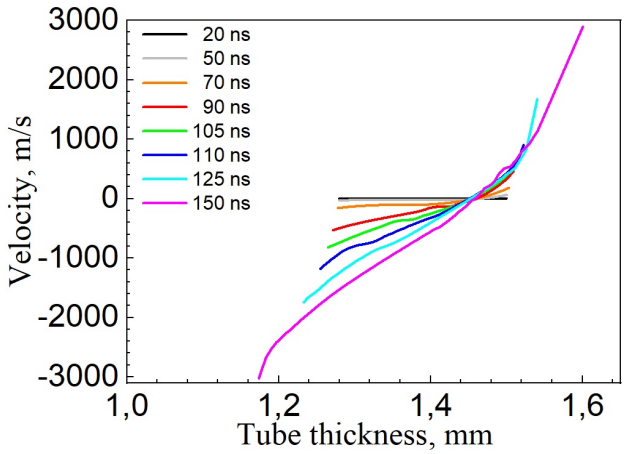

Fig.7. Velocity distribution over the tube thickness at different instants.

4. Conclusion

Numerical modeling of the processes occurring in a thick-walled tube made of stainless steel during the passage of a powerful current pulse through it has been performed. Using such a tube model, the evolution of the MITL parameters at high linear current densities was simulated.

It is found that the calculation results agree with the experimental data. So, on the experimental time dependence of the voltage measured on the inner surface of the tube, and on the same dependence obtained in the calculations, there is a feature with a lower rise rate of voltage. According to the numerical simulation, it was found that this feature corresponds to the melting wave reaching the inner surface of the tube and the completion of the melting process.

Acknowledgement

This work was supported by the Russian Foundation for Basic Research (project no. 20-21-00082).

5. References

[1] Aleksandrov V.V., Grabovsky E.V., Laukhin Ya.N., Mitrofanov K.N., Oleinik G.M., Predkova E.I., Reshetnyak O.B., Tkachenko S.I. Frolov I.N., *Plasma Phys. Rep.*, **48**, 101, 2022; doi: 10.1134/S1063780X22020015

[2] Grabovski E.V., Levashov P.R., Oleinik G.M., Olson C.L., Sasorov P.V., Smirnov V.P., Tkachenko S.I., Khishchenko K.V., *Plasma Phys. Rep.*, **32**, 718, 2006; doi: 10.1134/S1063780X06090029
[3] Tkachenko S.I., Grabovskii E.V., Kalinin Yu.G., Oleinik G.M., Aleksandrov V.V., Khishchenko K.V., Levashov P.R., Ol'khovskaya O.G., *Izv. Vyssh. Uchebn. Zaved., Fiz.* **57** (12–2), 279, 2014.
[4] Aleksandrov V.V., Branitskii A.V., Grabovskii E.V., Oleinik G.M., Predkova E.I., Samokhin A.A., Tkachenko S.I., Frolov I.N., Khishchenko K.V., Shishlov A.O., *Plasma Phys. Rep.*, **47**, 355, 2021; doi: 10.1134/S1063780X21040024
[5] Anisimov S.I., Imas Ya.A., Romanov G.S., Khodyko Yu.V., *Action of High-Power Radiation on Metals* (Springfield: National Technical Information Service, 1971).
[6] Fortov V.E., Khishchenko K.V., Levashov P.R., Lomonosov I.V., *Nucl. Instr. Meth. Phys. Res.* A, **415**(3), 604, 1998; doi: 10.1016/S0168-9002(98)00405-7
[7] *Knoepfel H. Pulsed High Magnetic Fields. Physical Effects and Generation Methods Concerning Pulsed Fields up to Megaoersted Level*. (London: North-Holland, 1970).
[8] Oleinik G.M., Aleksandrov V.V., Branitskii A.V., Frolov I.N., Grabovskii E.V., Predkova E.I., Reshetnjak O.B., Tkachenko S.I.*, Proc. of 8th Int. Cong. on Energy Fluxes and Radiation Effects, 2–8 October*, Tomsk, 2022; doi: 10.56761/EFRE2022.S2-O-009807